Local Binary Patterns versus Signal Processing Texture Analysis. A Study from a Performance Evaluation Perspective

Ovidiu Ghita[a], Dana E. Ilea[a], Antonio Fernandez[b] and Paul F. Whelan[a]

[a]Vision Systems Group, School of Electronic Engineering

Dublin City University, Dublin 9, Ireland

[b]Department of Engineering Design, School of Industrial Engineering

University of Vigo, Campus Universitario, 36310 Vigo, Spain

Abstract

Traditionally texture analysis is approached either by statistically evaluating the distribution of the pixels in a local neighbourhood or by filtering the image with a bank of filters that are applied to capture the changes in the spatial/frequency domain. The aim of this paper is to review and provide a detailed performance evaluation of a number of texture descriptors that analyse texture at micro-level such as Local Binary Patterns (LBP) and a number of standard filtering techniques that sample the texture information using either a bank of isotropic filters or Gabor filters. The experimental tests were conducted on standard databases where the classification results are obtained for single and multiple texture orientations. In our study we have also analysed the performance of standard filtering texture analysis techniques (such as those based of LM and MR8 filter banks) when applied to the classification of texture images contained in standard Outex and Brodatz databases.

Keywords: Texture classification, LBP, rotational invariance, Gabor filters, isotropic filters.

1. Introduction

Textured surfaces are an omnipresent characteristic of digital images and their precise identification plays an important role in the development of computer vision algorithms that target real-world applications. Although there is no widely accepted definition for texture, many image analysis approaches attempted to model this fundamental property in conjunction with the human visual system (HVS). In this regard, many psychophysical studies demonstrated that texture perception and interpretation is an early neural mechanism of the HVS which plays an important role in the process of figure-ground segmentation (Julesz, 1981; Bergen and Adelson, 1988; Balas, 2006). According to these studies, texture can be conceptualised as a statistical or geometric repetition of primitive descriptors (micro patterns) in the image and specific measures such as roughness, regularity, linearity, frequency, directionality, granularity and density can be employed to attain texture discrimination (one prominent example is the theory of textons that has been proposed by Julesz (Julesz, 1981) in the early 80s). While the surfaces of the imaged objects are often defined by an unbounded variety of textures, the task relating to the identification of the optimal texture analysis approach proved extremely challenging and the substantial efforts devoted by the vision community in the field of texture analysis were justified, as the availability of a robust texture descriptor will be extremely beneficial for a large spectrum of applications (Manjunath and Ma, 1996; Kovalev et al, 2001; Mäenpää et al, 2003; Nammalwar et al, 2003; Ghita et al, 2005; Rodriguez and Marcel, 2006; Xie and Mirmehdi, 2007; Tosun and Demir, 2011). Due to its intrinsic complexity, this fundamental image property has been researched for a number of decades and there is a large degree of consensus among vision researchers that texture analysis can be divided into four major categories: statistical, model-based, signal processing and structural, with statistical and signal processing techniques being the most investigated.

As indicated in numerous reviews on texture analysis (Chellappa et al, 1998; Materka and Strzelecki, 1998; Tuceryan and Jain, 1998; Zhang and Tan, 2002; Petrou and Sevilla, 2006), statistical approaches evaluate the spatial distribution of the pixels in the image by calculating features using first and second–order statistics (Haralick, 1979; Dyer et al, 1980; Haley and Manjunath, 1999). Among statistical texture analysis techniques the most investigated are based on the evaluation of the grey-level differences (first

order statistics) and co-occurrence matrices (second order statistics). These techniques are viewed as "historical" approaches to texture analysis and since their introduction they have been further advanced to improve either their discriminative power or their computational cost (Tsatsanis and Giannakis, 1992; Valkealahti and Oja, 1998). More recently the research focus has been on signal processing-based texture analysis methods. With these techniques, the image is typically filtered with a bank of filters of differing scales and orientations in order to capture the changes between specific frequency bands in the analysed image (Coggins and Jain, 1985; Haley and Manjunath, 1999; Liu and Wang, 2003). Early studies attempted to analyse the texture in the Fourier domain (Weszka et al, 1976), but these approaches were clearly outperformed by techniques that either analyse the texture using multi-channel narrow band Gabor filters or perform texture decomposition using the wavelet representation (Mallat, 1989; Porter and Canagarajah, 1997; Weber and Casasent, 2001). The multi-channel texture decomposition approach was firstly introduced by Jain and Farrokhnia (Jain and Farrokhnia, 1991) when they applied dyadic Gabor filters (Daugman, 1988; Kamarainen et al, 2006) to extract the textural features from images defined by oriented patterns. Arising from the experimental results, the authors conclude that the spectral information sampled by the narrow-band filters is sufficient to robustly discriminate between different textures in the image. Other studies have shown that the Gabor representation is optimal in the sense of minimising the uncertainties in space/frequency decomposition (Daugman, 1988; Bovik et al, 1990; Dunn et al, 1995; Dunn and Higgins, 1995; Kachouie and Alirazae, 2005), but the main practical problem with this approach is the onerous computational cost required to filter the image with a large bank of filters. To address this issue, Randen and Husoy (Randen and Husoy 1999a; Randen and Husoy, 1999b) proposed a methodology to compute optimised narrow-band filters and they evaluated their performance with respect to complexity/feature separation on a large number of test images. A conceptually related technique was proposed by Manjunath and Ma (Manjunath and Ma, 1996) where they attempted to minimise the redundancies generated by the non-orthogonal Gabor wavelets in the implementation of adaptive texture descriptors for browsing and image retrieval. A distinct alternative to address the limitations associated with the standard multi-channel texture decomposition based on Gabor filters resides in the construction of a universal dictionary of textons which can be regarded as textural primitives that are able to describe any digital image. Building on this concept, Leung and Malik (Leung and Malik, 2001) were among the

first to apply the texton-based representation to texture classification/recognition. In their work, the textons are calculated by clustering the responses of the filter bank (in this paper it is referred to as LM filter bank) into a set of prototype vectors that sample the principal texture characteristics. To this end, the authors proposed a bank of 48 filters that consist of a set of 36 oriented filters and 12 isotropic filters and the resulting textons were evaluated in the context of texture recognition. The experimental data proved the efficiency of this approach (97% detection rate) and due to its sound theoretical foundation this texture decomposition scheme has been further developed by other researchers. In this regard, Varma and Zisserman in (Varma and Zisserman, 2002; Varma and Zisserman, 2004) redeveloped the LM filter bank by retaining only the maximum responses returned by the oriented filters at each scale, a fact that allowed the implementation of a rotational invariant filter bank (which was referred to as MR8). In their paper the authors performed a large number of experiments to identify the optimal filter bank and they conclude that rotational invariance can be achieved at the expense of a marginal decrease in classification accuracy. A related approach that also addressed the texton-based texture analysis was proposed by Cula and Dana (Cula and Dana, 2004) where the authors applied bi-directional feature histograms for 3D texture recognition.

A recent direction of research in the field of texture classification attempted to bridge the concepts behind statistical and geometric texture analysis approaches. As indicated earlier, the statistical texture analysis evaluate the first and second order statistics of the intensities and pixel positions in the image, whereas geometrical approaches regard the texture as the spatial arrangement of textural primitives. While at the first glance the statistical and geometric texture analysis methods appear antagonistic, several researchers (Ojala et al, 1994; Ojala et al, 2001; Ojala et al, 2002a; Ojala et al, 2002b; Rodriguez and Marcel, 2006; Petrou and Sevilla, 2006; Nammalwar et al, 2010) observed that these approaches have strong complementary characteristics that allow modelling the macro-texture as the distribution of micro textural descriptors (or texture units). In this regard, the introduction of the Local Binary Patterns (LBP) concept by Ojala et al in 1994 has represented a milestone in texture analysis. This assertion is motivated not only by the sheer amount of LBP-related research published in the literature (according to the http://www.cse.oulu.fi/MVG/LBP_Bibliography website 1047 papers were published on the topic of LBP), but also by the vast spectrum of application domains that were well served by the LBP-based

texture analysis approach. Based on these compelling arguments, there is no doubt that LBP is one of the most researched areas in the field of texture analysis and it is the main objective of this paper to review this texture modelling approach from a theoretical and practical perspective. To further elevate the relevance of this paper, in this work we also assess the intrinsic characteristics of the LBP and mainstream signal processing texture analysis methods with a view of finding the commonalities (and differences) between these fundamental approaches in the process of texture modelling. Thus, in this paper we provide a detailed study that evaluates the performance of the LBP technique and a number of signal processing techniques that filter the image data with a bank of isotropic filters (Schmid, 2001), Gabor filters (Bovik et al, 1990; Dunn and Higgins, 1995) and texture analysis techniques that model the texture as a distribution of textons (Leung and Malik (LM) and Maximum Response (MR8) filter banks) (Leung and Malik, 2001; Varma and Zisserman, 2002; Varma and Zisserman, 2004). In the experimental section of this paper, the aforementioned techniques are evaluated on standard databases where the classification rate is calculated for one texture orientation and for multiple texture orientations. While the detailed performance evaluation represents the major contribution associated with this work, we would like to mention other novel aspects associated with our investigation that we believe are of interest to the computer vision research community. In particular we would like to mention the in-depth evaluation of the effects of image interpolation in the calculation of the standard LBP texture unit, which helped us to clarify several issues relating to the drop in classification that is characteristic for rotational invariant (RI) LBP forms. To further emphasise the link between classification accuracy and rotation invariance, in this paper we also provide comparative experimental results between texture classification schemes based on standard Gabor filtering and symmetrical (S) filters. Last but not least, a novel aspect associated with this work also reside in the detailed discussion of the experimental results that advance conclusions in regard to the process employed by the LBP and signal processing techniques in the process of sampling the texture in digital images.

This paper is organised as follows. Section 2 presents the texture extraction techniques evaluated in this study. Section 3 details the experimental results, while in Section 4 the classification results are analysed and discussed. Section 5 concludes this paper.

2. Methods

2.1 Local Binary Patterns (LBP) Texture Extraction

The Local Binary Patterns (LBP) concept, as developed by Ojala et al (Ojala et al, 2002a), attempts to decompose the texture into small units where the texture features are defined by the distribution (histogram) of the LBP values calculated for each pixel in the image. The concept behind LBP is appealing since the LBP distributions are suitable to sample the textural properties in the homogenous image regions irrespective to their sizes. The LBP texture unit is calculated in a 3×3 square neighbourhood by applying a simple threshold operation with respect to the central pixel as illustrated in equation (1).

$$T = \{t(g_0 - g_c),...,t(g_{P-1} - g_c)\}, \qquad t(x) = \begin{cases} 1 & x \geq 0 \\ 0 & x < 0 \end{cases} \tag{1}$$

where T is the texture unit, g_c is the grey level value of the central pixel, g_P are the grey level values of the pixels adjacent to the central pixel in the 3×3 neighbourhood, P defines the number of pixels in the 3×3 neighbourhood and function $t(.)$ defines the threshold operation. For a 3×3 neighbourhood the value of P is 8. To encompass the spatial arrangement of the pixels in the 3×3 neighbourhood, the LBP value for the tested (central) pixel is calculated using the following relationship:

$$LBP = \sum_{i=0}^{P-1} t(g_i - g_c) * 2^i \tag{2}$$

where $t(g_i - g_c)$ is the value of the thresholding operation illustrated in equation (1). The LBP values calculated using equation (2) are in the range [0,255].

As the LBP values do not measure the greyscale variation, the LBP is commonly used in conjunction with a contrast measure C. In our implementation, the contrast measure C, as suggested by Ojala et al (Ojala et al, 2002a), is calculated as the normalized difference between the grey levels of the pixels with a value of 1 and the pixels with a value of 0 in the texture unit T (see equation 1). The distribution of the LBP/C values calculated for all pixels in the image represents the texture spectrum. The LBP/C distribution can be defined as a histogram of size $256 + b$, where the first 256 bins are required by the distribution of the LBP values and the last b bins of the distribution are required to sample the quantized

contrast measure. In practice, the contrast measure is sampled in 4, 8 or 16 bins to obtain a compact descriptor. Fig. 1 illustrates the LBP and contrast distributions for three differently textured images (top – oriented texture, middle – mildly oriented texture and bottom – isotropic texture).

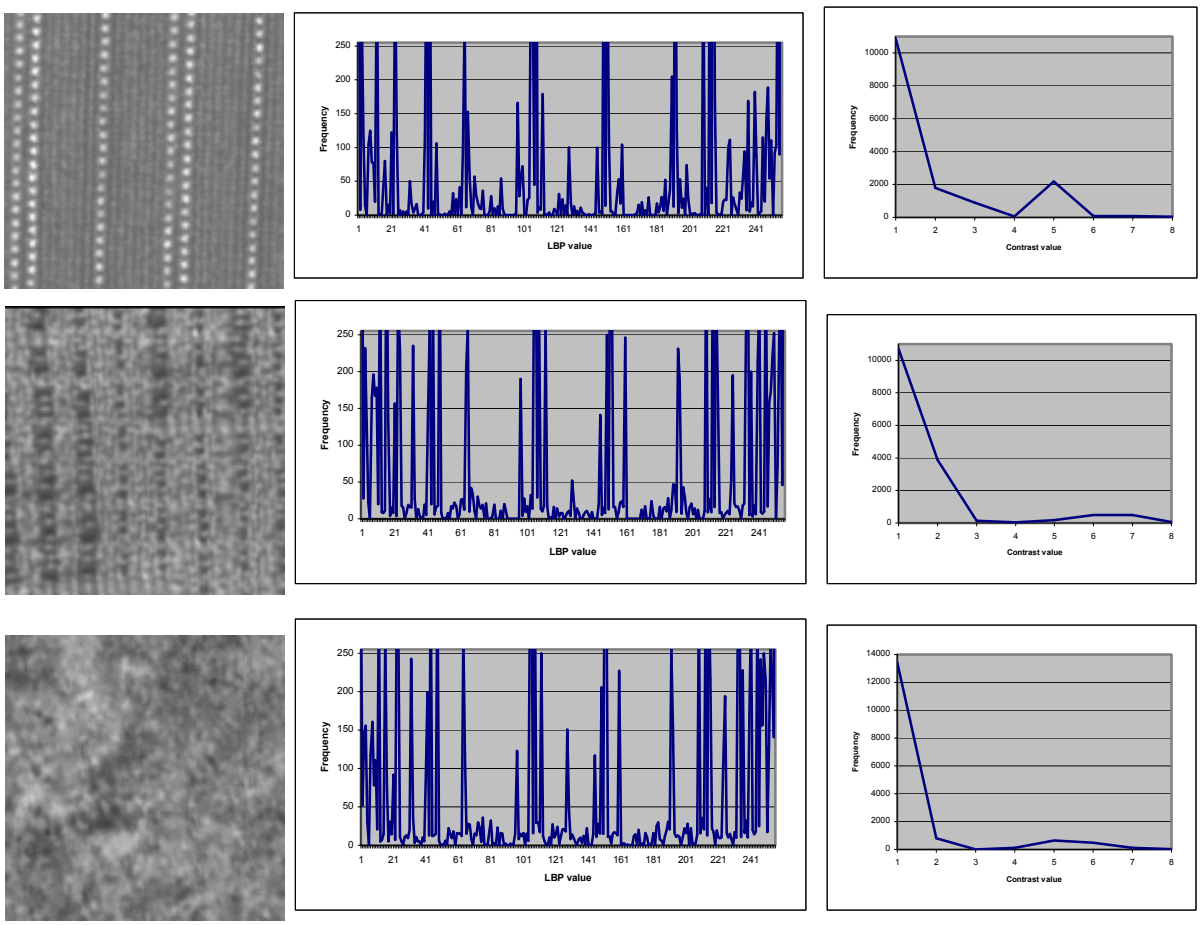

Fig. 1. The LBP and contrast (quantization level 8) distributions calculated for thereof the textures (Ojala et al, 2002b) used in our experiments.

2.2. Rotational Invariant (RI) LBP Descriptors

The LBP values calculated for each texture unit using equation (2) are sensitive to texture orientation. This is motivated by the fact that the standard LBP descriptor encompasses the spatial distribution of the pixels along with the distribution of the intensity values within a square 3×3 neighbourhood. While this property may be useful when this texture descriptor is included in the development of applications such as inspection of surfaces defined by oriented textures, it is a considerable drawback when this image descriptor is used for texture classification. To address this problem, Ojala et al (Ojala et al, 2002a)

proposed to modify the LBP descriptor in order to achieve rotation invariance (RI). To remove the sensitivity to rotation, the texture descriptor has to be calculated within a circular neighbourhood and the texture should be evaluated in terms of uniformity. Since the pixels in the image are organised as a discrete matrix, the pixels situated within the circular neighbourhood are not positioned exactly on the image grid and their values are calculated by using bilinear interpolation. To enforce the concept of uniformity in the calculation of the LBP values, Ojala et al (Ojala et al, 2002a) introduced the term "uniform patterns" that is defined in terms of the number of transitions between 0 and 1 in the LBP mask obtained after thresholding the pixels from the circular neighbourhood with the intensity value of the central pixel. In this way, they defined a pattern as uniform if the binary LBP pattern has a maximum of two transitions; otherwise the pattern is classed as non-uniform. For instance, if the LBP value is calculated in a circular 8 neighbourhood, the binary patterns 00000000, 00000001, 00000011, 00001000,…, 11111111 are classed as uniform, while patterns such as 01100101, 10101000, 01101101,…, 10101010 are classed as non-uniform (see Fig. 2).

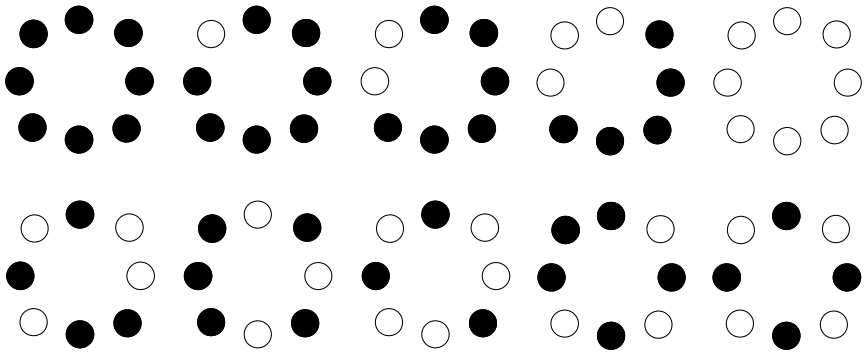

Fig. 2. LBP masks obtained after the application of the thresholding operation. The pixels that return the value 0 in equation (1) are marked in the diagram with a black disc while the pixels that generate a value 1 are marked with a white disc. (Top row) Examples of uniform patterns (maximum of two transitions in the binary pattern). (Bottom row) Examples of non-uniform patterns.

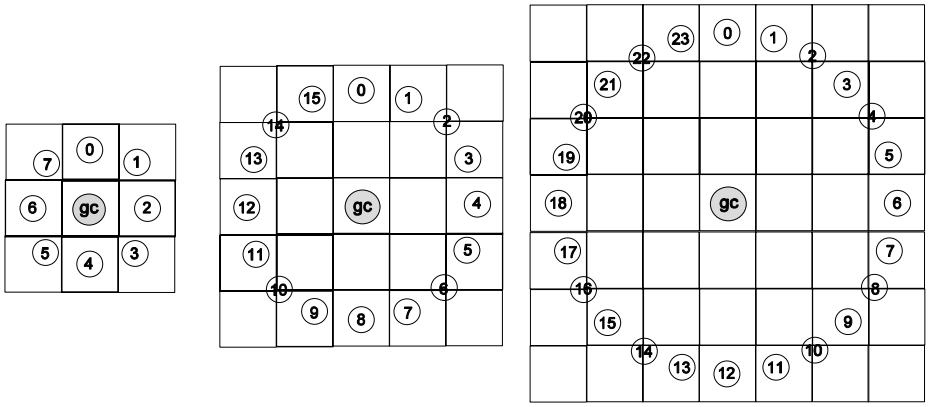

(a) (b) (c)

Fig. 3. LBP^{ri} pattern sizes. (a) P=8, R=1. (b) P=16, R=2. (c) P=24, R=3.

As indicated earlier, the idea behind uniformity concept is to group the non-uniform patterns in a distinct class while the values for uniform patterns are given by the total number of elements with a value 1 in the binary LBP pattern (see equation 5). In the original implementation (Ojala et al, 2002a), the rotational invariant (RI) LPB descriptors are calculated for neighbourhoods with different sizes (see Fig. 3) as follows:

$$T_r(g_m, g_n) = \left| t(g_m - g_c) - t(g_n - g_c) \right| \tag{3}$$

$$U_{P,R} = T_r(g_{P-1}, g_0) + \sum_{i=1}^{P-1} T_r(g_i, g_{i-1}) \tag{4}$$

$$LBP_{P,R}^{ri} = \begin{cases} \sum_{i=0}^{P-1} t(g_i - g_c) & if \quad U_{P,R} \le 2 \\ P+1 & Otherwise \end{cases} \tag{5}$$

where P is the number of pixels in the LBP mask, R is the radius of the mask, *ri* indicates that the LBP value is rotational invariant, $T_r(g_m,g_n)$ defines the transition between pixels with indexes m and n and $U_{P,R}$ is the function that evaluates the uniformity of the binary LBP pattern.

To improve its discriminative power, the LBP^{ri} value is complemented with the contrast measure C that is calculated as the variance of the pixels situated in the LBP mask (Ojala et al, 2002a).

2.3. Multi-channel Texture Decomposition Using Gabor Filtering

There has been a widely accepted consensus among vision researchers that filtering an image with a large number of oriented band pass filters such as Gabor is an optimal approach to analyse texture (Bovik et al, 1990; Porter and Canagarajah, 1997; Lahajnar and Kovacic, 2003; Ilea and Whelan, 2008). This is motivated by the fact that this approach extracts the texture features over the entire spectrum of frequencies by filtering the image with a bank of Gabor filters calculated for different scales and orientations. This operation performs multi-channel texture decomposition and this is usually achieved by filtering the input textured image with a dyadic two-dimensional (2D) Gabor filter bank that was initially suggested by Daugman (Daugman, 1988) and later applied to texture segmentation by Jain and Farrokhnia (Jain and Farrokhnia, 1991). The 2D Gabor function that is used to implement the even-symmetric 2D discrete filters can be written as:

$$h_{\sigma,\lambda,\varphi}(x,y) = \exp(-\frac{x'^2 + y'^2}{2\sigma^2})\cos(\frac{2\pi x'}{\lambda} + \varphi) \ , \ f_0 = \frac{1}{\lambda} \tag{6}$$

$$B = \log_2\left(\frac{\pi\sigma f_0 + \sqrt{\ln(2)/2}}{\pi\sigma f_0 - \sqrt{\ln(2)/2}}\right) \tag{7}$$

where $x' = x\cos\theta + y\sin\theta$, $y' = -x\sin\theta + y\cos\theta$ and B is the bandwidth of the filter. In equation (6) the parameter σ is the scale of the Gabor filter, θ is the orientation, λ is the wavelength of the cosine function that is given in pixels and $f_0=1/\lambda$ is the frequency parameter that controls the number of cycles of the cosine function within the envelope of the 2D Gaussian (φ is the phase offset and it is usually set to zero to implement 2D even-symmetric filters). Based on the formulation illustrated in equation (6) it can be deduced that the Gabor filters are band pass filters where the parameters σ, θ, $1/\lambda$ determine the sub-band that is covered by the Gabor filter in the spatial-frequency domain. In practice, the parameters of the Gabor filters are chosen to optimise the trade-off between spectral selectivity (texture decomposition) and the size of the bank of filters. Typically, the central frequencies are selected to be one octave apart (i.e. $\log_2(f_{i+1}/f_i) = 1$) and for each central frequency a set of filters corresponding to four (0^0,45^0,90^0,135^0) or six orientations (0^0,30^0,60^0,90^0,120^0,150^0) is constructed. To illustrate the spectral selectivity of the Gabor filters, in Fig. 4 a number of Gabor filters with different values for σ, θ and f_0 parameters are illustrated.

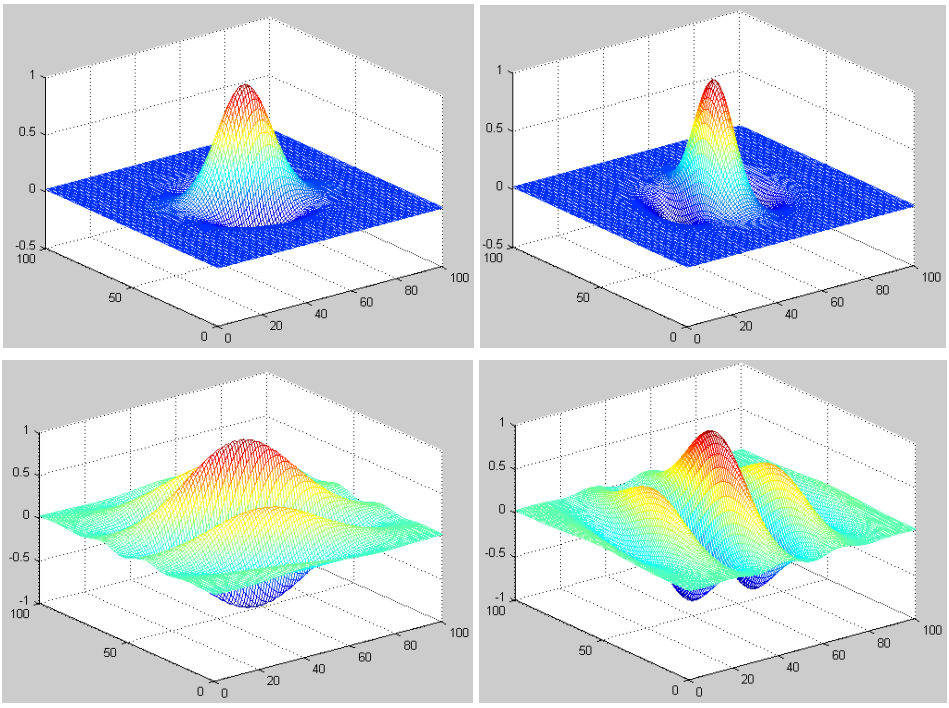

Fig. 4. 2D Gabor filters for 30^0 and 120^0 orientations. (Top row) scale σ =1.0, central frequency f_0=1.5/2π. (Bottom row) Scale σ =2.0, central frequency f_0=2.5/2π.

2.4. Multi-channel Texture Decomposition Using Isotropic Gabor Filters

The main disadvantage associated with approaches based on multi-channel texture decomposition using a large bank of Gabor filters is the large computational cost. Thus, to limit the number of orientations in the Gabor filter bank it would be advantageous if the filters would have isotropic characteristics (i.e. rotational invariant filters). Using this concept, Schmid (Schmid, 2001) developed a set of rotational invariant Gabor-like filters (in this work they are referred to as symmetrical (S)-Filters) that were applied to construct texture models for image retrieval. The S-Filters proposed in (Schmid, 2001) are constructed as follows,

$$S_{\tau,\sigma}(x,y) = S_o(\tau,\sigma) + \cos\left(\frac{\pi\tau\sqrt{x^2+y^2}}{\sigma}\right)\exp\left(-\frac{x^2+y^2}{2\sigma^2}\right) \tag{8}$$

where τ is the frequency parameter that controls the number of cycles of the cosine function within the Gaussian envelope, σ is the scale parameter and the term S_0 is added to remove the DC component of the

2D S-Filter. The parameters τ and σ can be adjusted to capture a particular sub-band in the spatial-frequency domain as illustrated in Fig. 5.

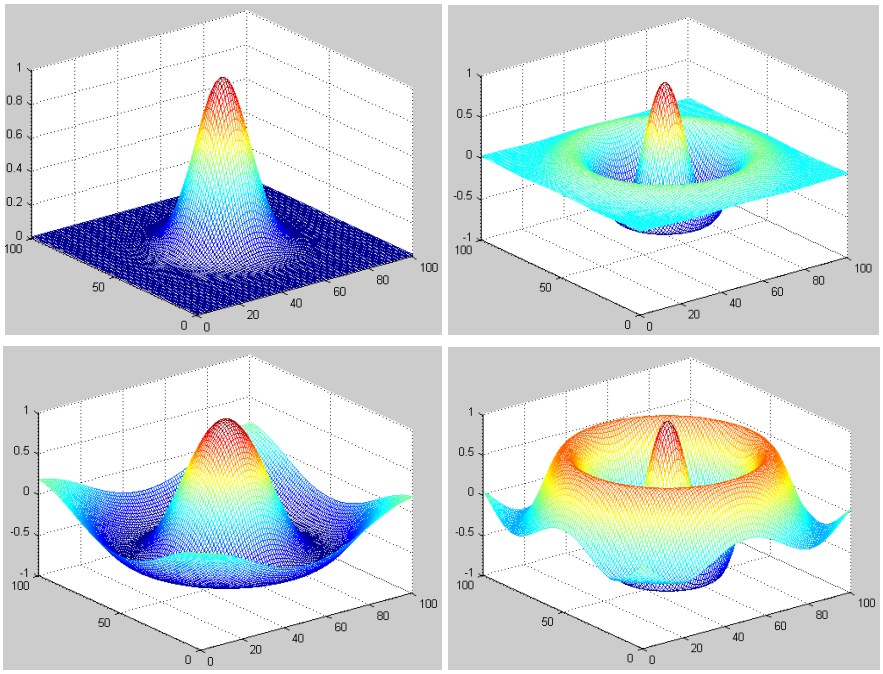

Fig. 5. 2D S-Filters constructed using the following (σ,τ) parameters: (a) (1,0). (b) (2,1). (c) (4,1) and (d) (4,2).

3. Experiments and Results

The aim of this section is to provide a comparative study between the performances in texture classification offered by the LBP texture descriptors and the standard signal processing texture analysis techniques based on Gabor filters and S-Filters. To evaluate the performance of the texture extraction techniques based on filtering the image with large banks of oriented filters, additional experiments were conducted using the LM and MR8 filtering approaches and the results are also reported in this paper for completeness. In particular we were interested in evaluating the influence of the image size and the texture rotation on the classification results. In order to perform these measurements, we have applied the LBP texture descriptors in both the standard and rotational invariant forms. The experimental results reported in this paper were conducted on four Outex databases (TC 00000, TC 00001, TC 00002, TC 00010) (Ojala et al, 2002b) and on Brodatz (Brodatz, 1966) database. The Outex databases are formed by 24 classes of standard textures as illustrated in Fig. 6 (canvas, carpet and tile).

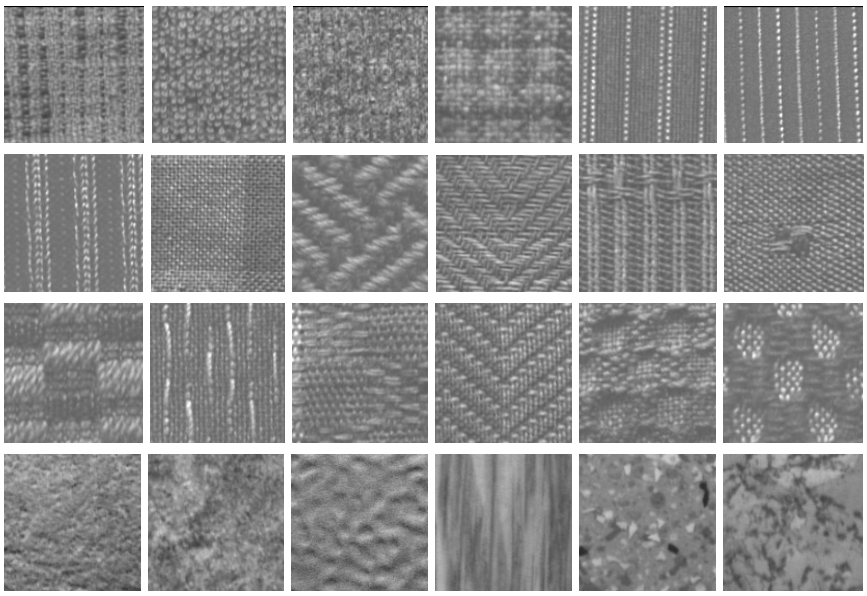

Fig. 6. Samples of the 24 textures contained in the Outex (Ojala et al, 2002b) databases.

Database TC 00000 comprises of 480 texture images with a single orientation with an image size of 128×128. Database TC 00001 is formed by splitting the images that form the database TC 00000 in four (this results in 2112 texture images where the image size is 64×64). Database TC 00002 is obtained in a similar fashion by splitting the texture images of database TC 00001 into four parts (this results in 8832 images where the image size is 32×32). The databases TC 00000, 00001 and 00002 were generated using a single texture orientation and they were included in this study to evaluate the robustness of the analysed texture extraction techniques to variations in image size. Database TC 00010 is generated by capturing the textures that form the database TC 00000 with nine rotation angles (0^0, 5^0, 10^0, 15^0, 30^0, 45^0, 60^0, 75^0, 90^0) and is formed by 4320 images where the image size is 128×128 (for more details in regard to the construction of the Outex databases the reader can refer to (Ojala et al, 2002b)).

The Brodatz database (Brodatz, 1966) used in our study consists of 36 texture images. This database is formed by near-isotropic textures captured with a single orientation and the original images were split in 4 (database BD 00000), 16 (database BD 00001) and 64 sub-images (database BD 00002). Database BD 00000 comprises 144 non-overlapped texture images (image size: 256×256), database BD 00001 consists of 576 non-overlapped texture images (image size: 128×128) and database BD 00002 comprises 2304

non-overlapped texture images (image size: 64×64). Fig. 7 depicts the 36 classes of the Brodatz textures used in our experiments.

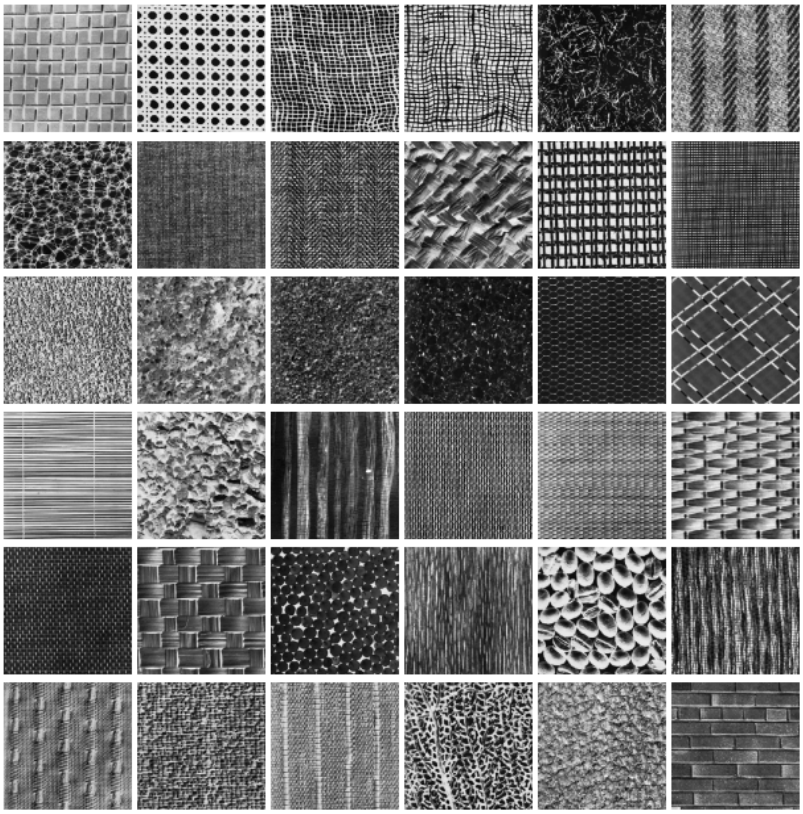

Fig. 7. The 36 textures from the Brodatz (Brodatz, 1966) database used in our experiments.

3.1. Classification Procedure

In our experiments the similarity between the training and test datasets is evaluated using the SVM classification scheme (Chang and Lin, 2001). Since the texture analysis algorithms published in the vision literature employ different classification algorithms to evaluate the robustness of the texture descriptors, this fact renders the analysis with respect to classification accuracy extremely difficult. To circumvent this issue, we have adopted the SVM classification scheme since its implementation is standard and readily available (Chang and Lin, 2001) and the results reported in this paper can be easily benchmarked against the results obtained by other texture analysis algorithms. To avoid the computational problems associated with complex classification models (such as the optimisation of a large set of parameters), in our implementation we have used polynomial kernels to map the feature space. The first tests were

conducted on texture databases formed by non-rotated texture images. In our experiments half of the images were used for training and the remaining half were used for testing.

To evaluate the robustness to image rotation of the algorithms detailed in this paper, we have conducted a number of experiments on database TC 00010 that comprises texture images captured with 9 rotation angles. In order to sample the effect of image rotation we have adopted the approach suggested by Ojala et al (Ojala et al, 2002a) where the classifier was trained with 480 images captured with the standard orientation (angle 0^0) while the images with the remaining (rotated) orientations were used for testing. Training the classifier with a single orientation is the optimal strategy to assess the robustness of the evaluated techniques to image rotation since no bias in classification is introduced.

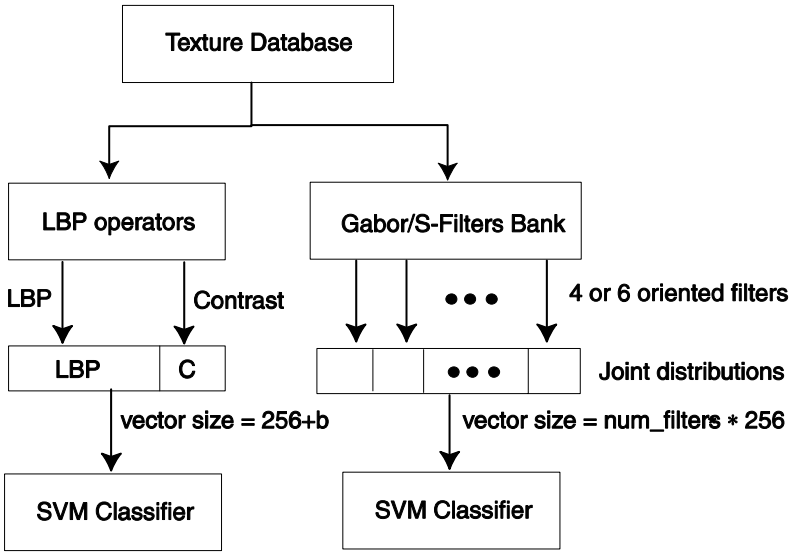

Fig. 8. Training process.

The training process is illustrated in Fig. 8 and it can be noticed that the classifier is trained with feature vectors that define either the LBP/C distributions (size: 256+b, where 256 is the size of the LBP distribution and *b* is the quantisation level of the contrast measure) or by the distributions calculated from the responses obtained after filtering the texture images with the multi-channel filter banks (in our implementation we have normalized the intensity values of the filtered images in the range [0,255] and as a result the size of the feature vector is: 256×*num_filters*, where *num_filters* defines the number of filters in the filter bank).

3.2. Classification Results for the LBP Technique

In this section we evaluate the classification accuracy returned by the Local Binary Patterns (LBP) technique where the operators were used in both the standard and rotational invariant forms. In this study the standard LBP descriptor and the rotational invariant $LBP^{ri}_{8,1}$, $LBP^{ri}_{16,2}$, $LBP^{ri}_{24,3}$ texture descriptors are evaluated.

Table 1. Experimental results for the LBP descriptors with respect to image size.

Database	Method	Accuracy [%]
TC 00000 (128×128)	LBP/C Bins = 4	100
	LBP/C Bins = 8	100
	LBP/C Bins = 16	97.91
	$LBP^{ri}_{8,1}$	92.50
	$LBP^{ri}_{16,2}$	87.91
	$LBP^{ri}_{24,3}$	86.25
	LBP^{ri}_{MR}	92.91
TC 00001 (64×64)	LBP/C Bins = 4	98.48
	LBP/C Bins = 8	98.48
	LBP/C Bins = 16	98.86
	$LBP^{ri}_{8,1}$	91.85
	$LBP^{ri}_{16,2}$	90.24
	$LBP^{ri}_{24,3}$	91.38
	LBP^{ri}_{MR}	97.15
TC 00002 (32×32)	LBP/C Bins = 4	92.32
	LBP/C Bins = 8	93.59
	LBP/C Bins = 16	94.47
	$LBP^{ri}_{8,1}$	77.89
	$LBP^{ri}_{16,2}$	73.05
	$LBP^{ri}_{24,3}$	67.50
	LBP^{ri}_{MR}	87.54
BD_00000 (256×256)	LBP/C Bins = 4	95.83
	LBP/C Bins = 8	100
	LBP/C Bins =16	100
	$LBP^{ri}_{8,1}$	94.44
	$LBP^{ri}_{16,2}$	93.05
	$LBP^{ri}_{24,3}$	93.05
	LBP^{ri}_{MR}	95.83
BD_00001 (128×128)	LBP/C Bins = 4	99.65
	LBP/C Bins = 8	99.65
	LBP/C Bins = 16	100
	$LBP^{ri}_{8,1}$	100
	$LBP^{ri}_{16,2}$	98.95
	$LBP^{ri}_{24,3}$	97.22
	LBP^{ri}_{MR}	99.65
BD_00002 (64×64)	LBP/C Bins = 4	96.87
	LBP/C Bins = 8	96.87
	LBP/C Bins = 16	96.79
	$LBP^{ri}_{8,1}$	94.44
	$LBP^{ri}_{16,2}$	94.36
	$LBP^{ri}_{24,3}$	93.23
	LBP^{ri}_{MR}	95.75

Table 2. Experimental results for the LBP descriptors with respect to texture rotation.

Database	Method	Accuracy [%]
TC 00010 (128×128)	LBP/C Bins = 4	63.69
	LBP/C Bins = 8	69.42
	LBP/C Bins = 16	71.30
	$LBP^{ri}_{8,1}$	84.66
	$LBP^{ri}_{16,2}$	87.50
	$LBP^{ri}_{24,3}$	85.23
	LBP^{ri}_{MR}	89.68

As indicated in Section 3.1 these experiments were performed using four Outex databases (TC 00000, TC 00001, TC 00002, TC 00010) and three Brodatz databases (BD 00000, BD 00001 and BD 00002) and the classification results are illustrated in Tables 1 and 2 (in these tables the parameter *bins* indicates the quantization level for the contrast measure and LBP^{ri}_{MR} denotes that the rotational invariant LBP operator has been applied in the multi-resolution form – the construction of this texture descriptor will be explained later in this section).

The results illustrated in Tables 1 and 2 are quite interesting and require a more detailed analysis. For instance, it can be observed that the standard LBP/C operator provides excellent discrimination when the classifier is trained and tested on texture images defined by a single orientation, but its discriminative power is substantially diminished even when dealing with small texture rotations. Table 2 shows that the rotational invariant (RI) LBP operators are more robust to handle texture rotation. But it is useful to note that the discriminative power of these descriptors when applied to non-rotated textures is significantly lower than that of the standard LBP/C texture descriptor especially when applied to small images defined by oriented textures (database TC 00002). Thus, the question that immediately arises is what causes the drop in classification accuracy for rotational invariant descriptors when applied to non-rotated texture databases? To answer this question we need to revisit Section 2.2 where the calculation of these rotational invariant descriptors is presented. In our opinion, this drop in classification can be caused by two factors, *either* by the image interpolation that is applied to calculate the intensity values of the pixels in the circular neighbourhood that are not positioned exactly on the image grid *or* by the poor discriminative power offered by the "uniform" patterns (we recall that the non-uniform patterns are labelled with the

same value P+1). To clarify the impact of the interpolation procedure on the discriminative power of the LBP descriptors, in this paper we propose an approach that implements a new LBP/C operator where the LBP value is calculated within the circular pattern (P=8, R=1) illustrated in Fig 3(a). The LBP values for the *circularly* symmetric texture unit are calculated using equation (2) and the new operator is referred to as LBP_C8. The classification results obtained when this new texture descriptor (LBP_C8) is employed are illustrated in Table 3.

Table 3. Experimental results for the LBP_C8 texture descriptor.

Database	Method	Accuracy [%]
TC 00000 (128×128)	LBP_C8 Bins = 4	100
	LBP_C8 Bins = 8	100
	LBP_C8 Bins = 16	97.50
TC 00001 (64×64)	LBP_C8 Bins = 4	99.05
	LBP_C8 Bins = 8	99.24
	LBP_C8 Bins = 16	99.24
TC 00002 (32×32)	LBP_C8 Bins = 4	93.63
	LBP_C8 Bins = 8	94.97
	LBP_C8 Bins = 16	94.99
TC 00010 (128×128)	LBP_C8 Bins = 4	61.09
	LBP_C8 Bins = 8	68.02
	LBP_C8 Bins = 16	70.67
BD_00000 (256×256)	LBP_C8 Bins = 4	97.22
	LBP_C8 Bins = 8	97.22
	LBP_C8 Bins = 16	98.61
BD_00001 (128×128)	LBP_C8 Bins = 4	99.65
	LBP_C8 Bins = 8	99.65
	LBP_C8 Bins = 16	100
BD_00002 (64×64)	LBP_C8 Bins = 4	96.70
	LBP_C8 Bins = 8	96.79
	LBP_C8 Bins = 16	96.61

From the results outlined in Table 3 it can be concluded that image interpolation does not have a negative impact on the classification accuracy (in fact the classification results are even better than those obtained when the standard LBP/C descriptor was evaluated) and we can safely assume that the loss in discrimination associated with the rotational invariant LBP descriptors is caused by the relative weak discrimination offered by the "uniform" patterns in sampling the texture characteristics. This conclusion is also validated by the accurate classification results obtained when the RI LBP operators were applied to Brodatz databases (see Table 1) and these results are motivated by the fact that the Brodatz databases are

constructed using images defined by isotropic textures that would favour the rotational invariance associated with the RI LBP texture descriptors.

To further analyse the performance of the RI LBP operators, the next tests were conducted to evaluate whether the inclusion of the RI LBP operators into a multi-resolution classification approach would produce better results. To achieve this, we have concatenated the distributions that have been obtained when the RI LBP operators are calculated for all pattern sizes depicted in Fig. 3 ((P=8, R=1), (P=16, R=2) and (P=24, R=3)). The multi-resolution operator is referred to as LBP^{ri}_{MR} and the classification results when this operator has been applied to Outex and Brodatz databases are depicted in Tables 1 and 2. The experimental results indicate that the performance of the new multi-resolution operator is higher than the results attained when the RI LBP operators have been applied to texture databases at each resolution. The improved performance of the multi-resolution RI LBP operator is especially noticeable when applied to databases TC 00001, TC 00002 and TC 00010. Based on these experimental results we conclude that the discriminative power of the distribution of the "uniform" patterns improves dramatically when they are jointly analysed at different resolutions.

3.3. Classification Results for the Multi-channel Gabor Filtering Technique

In this section we evaluate the classification results achieved using the multi-channel texture decomposition technique detailed in Section 2.3. In our experiments we have filtered the input image with a small bank of filters with four (0^0, 45^0, 90^0, 135^0) and six (0^0, 30^0, 60^0, 90^0, 120^0, 150^0) orientations. The central frequency parameter was also varied by setting it to the values $1.0/2\pi$, $1.5/2\pi$, $2.0/2\pi$ and $2.5/2\pi$. Since the size of the texture images in databases TC 00001 and TC 00002 is relatively small, the standard deviation (scale) parameter was fixed to 1.0 to avoid the windowing errors caused by the convolution with large filters. The calculation of the Gabor filter bank using a small value of the scale parameter is also motivated by the fact that the LBP descriptors are calculated within a small neighbourhood and this will generate a fair scenario when their relative texture classification performances are evaluated. (It is important to note that in the implementation of large filter banks the values of the scale and the central

frequency parameters are selected to obtain an octave spaced filter bank.) The experimental tests were conducted on Outex and Brodatz databases as before and the classification results are outlined in Tables 4 and 5 (to limit the size of these tables the classification results for Brodatz databases are only reported for six orientation (6 angles) multi-channel texture decomposition).

Table 4. Experimental results for the Gabor filtering (GF) technique with respect to image size.

Database	Method	Accuracy [%]
TC 00000 (128×128)	GF $f_0 = 1.0/2\pi$, 4 angles	85.83
	GF $f_0 = 1.5/2\pi$, 4 angles	92.08
	GF $f_0 = 2.0/2\pi$, 4 angles	96.25
	GF $f_0 = 2.5/2\pi$, 4 angles	97.50
	GF $f_0 = 1.0/2\pi$, 6 angles	86.25
	GF $f_0 = 1.5/2\pi$, 6 angles	92.91
	GF $f_0 = 2.0/2\pi$, 6 angles	97.08
	GF $f_0 = 2.5/2\pi$, 6 angles	98.33
TC 00001 (64×64)	GF $f_0 = 1.0/2\pi$, 4 angles	83.99
	GF $f_0 = 1.5/2\pi$, 4 angles	90.62
	GF $f_0 = 2.0/2\pi$, 4 angles	96.96
	GF $f_0 = 2.5/2\pi$, 4 angles	98.20
	GF $f_0 = 1.0/2\pi$, 6 angles	84.75
	GF $f_0 = 1.5/2\pi$, 6 angles	91.47
	GF $f_0 = 2.0/2\pi$, 6 angles	97.72
	GF $f_0 = 2.5/2\pi$, 6 angles	98.95
TC 00002 (32×32)	GF $f_0 = 1.0/2\pi$, 4 angles	64.35
	GF $f_0 = 1.5/2\pi$, 4 angles	69.54
	GF $f_0 = 2.0/2\pi$, 4 angles	86.07
	GF $f_0 = 2.5/2\pi$, 4 angles	87.95
	GF $f_0 = 1.0/2\pi$, 6 angles	63.26
	GF $f_0 = 1.5/2\pi$, 6 angles	71.73
	GF $f_0 = 2.0/2\pi$, 6 angles	86.73
	GF $f_0 = 2.5/2\pi$, 6 angles	90.76
BD 00000 (256×256)	GF $f_0 = 1.0/2\pi$, 6 angles	86.11
	GF $f_0 = 1.5/2\pi$, 6 angles	91.66
	GF $f_0 = 2.0/2\pi$, 6 angles	97.22
	GF $f_0 = 2.5/2\pi$, 6 angles	100
BD 00001 (128×128)	GF $f_0 = 1.0/2\pi$, 6 angles	94.09
	GF $f_0 = 1.5/2\pi$, 6 angles	95.83
	GF $f_0 = 2.0/2\pi$, 6 angles	98.95
	GF $f_0 = 2.5/2\pi$, 6 angles	99.65
BD 00002 (64×64)	GF $f_0 = 1.0/2\pi$, 6 angles	86.73
	GF $f_0 = 1.5/2\pi$, 6 angles	93.58
	GF $f_0 = 2.0/2\pi$, 6 angles	95.92
	GF $f_0 = 2.5/2\pi$, 6 angles	96.61

Table 5. Experimental results for the Gabor filtering technique with respect to texture rotation.

Database	Method	Accuracy [%]
TC 00010 (128×128)	GF $f_0 = 1.0/2\pi$, 4 angles	79.01
	GF $f_0 = 1.5/2\pi$, 4 angles	68.28
	GF $f_0 = 2.0/2\pi$, 4 angles	64.03
	GF $f_0 = 2.5/2\pi$, 4 angles	60.72
	GF $f_0 = 1.0/2\pi$, 6 angles	79.14
	GF $f_0 = 1.5/2\pi$, 6 angles	68.88
	GF $f_0 = 2.0/2\pi$, 6 angles	64.50
	GF $f_0 = 2.5/2\pi$, 6 angles	63.15

The results depicted in Table 4 indicate that the best classification results are obtained when the texture features are extracted using filter banks with six orientations and the central frequency is set to large values. This observation is valid only for experiments carried out on databases that comprise non-rotated textures (TC 00000, TC 00001, TC 00002, BD 00000, BD 00001 and BD 00002). When the experiments were conducted using rotated textures (TC 00010) the best results are obtained when the central frequency parameter is set to low values. These results are surprising since we can notice a clear similarity with the results obtained when the LBP techniques were evaluated. In other words by lowering the value of the central frequency we simply filtered out the high frequency components from the texture spectrum and this is somewhat similar to the "uniformity" concept enforced in the calculation of the RI LBP distributions. Thus, the classification results show better performance in the presence of texture rotation. Nonetheless, when the value of the central frequency is increased, the Gabor filters approximate oriented operators and the direction of the texture plays a crucial role in the classification process.

3.4. Classification Results for the S-Filtering Technique

The S-Filters were introduced by Schmid (Schmid, 2001) to extract a set of rotational invariant texture features that can be used to model generic descriptors for image retrieval. The 2D S-Filters are constructed using equation (8) where the scale σ and frequency τ are the parameters that model the spectral sensitivity of these filters. In the original implementation (Schmid, 2001) the filter set has been constructed by varying the scale σ between 2 and 10 and τ between 0 and 4. In our implementation we have implemented a filter set using the following pairs for (σ, τ): (1,0), (2,1), (4,1), (6,2), (8,3), (10,4) and the experimental results are depicted in Table 6.

Table 6. Experimental results for the S-Filtering technique.

Database	Method	Accuracy [%]
TC 00000	S-Filtering	59.58
TC 00001		66.19
TC 00002		46.15
TC 00010		68.61
BD 00000		75.00
BD 00001		74.30
BD 00002		66.69

The results depicted in Table 6 indicate that the best results are obtained when this technique is applied to the database TC 00010 and Brodatz databases (this is motivated by the fact that the Brodatz textures have strong isotropic characteristics). In Table 6, it can be observed that the classification accuracy drops significantly when this texture analysis scheme is applied to small images (database TC 00002). We conclude that the texture features extracted by filtering the texture images with a bank of S-filters are suitable to discriminate isotropic textures, but are inefficient when applied to the classification of oriented textures, which is in line with the concept behind this texture analysis technique.

3.5. Classification Results for the LM and MR8 Filter Banks

While the texture analysis techniques based on filtering the input images with Leung and Malik (LM) (Leung and Malik, 2001) and Maximum Response (MR8) filter banks (Varma and Zisserman, 2004) are standard signal processing approaches that sample the texture characteristics using multi-channel filter banks, in this section we evaluate their performance when applied to Outex and Brodatz databases. The LM is a multi-scale, multi-orientation filter bank that consists of 48 filters (36 oriented and 12 isotropic). From these 48 filters, 36 are calculated using the first and second derivative of the Gaussian for 3 scales $(\sigma_x,\sigma_y) = \{(1,3), (2,6), (4,12)\}$, 6 orientations and 2 phases (to implement odd and even-symmetric filters), 8 isotropic filters are generated using the Laplacian of Gaussian (LoG) and the remaining 4 isotropic filters are calculated using the standard Gaussian. The MR8 filter bank is obtained by recording only the filter from the LM bank that generates the maximum response from all orientations for the symmetric and odd filters at each scale (for more details refer to Varma and Zisserman (Varma and Zisserman, 2002; Varma and Zisserman, 2004)). Thus, the MR8 filter bank is formed by 8 filters that implement a multi-scale rotational invariant filter bank (in the original implementation detailed in (Varma and Zisserman,

2004) only two isotropic filters were included in the construction of the MR8 filter bank, where the standard deviation for the Gaussian and LoG operators is set to 10 pixels). The experimental results when the LM and MR8 filter banks are applied to the Outex and Brodatz databases are depicted in Tables 7 and 8.

Table 7. Experimental results for the LM filter bank.

Database	Method	Accuracy [%]
TC 00000	LM - Filtering	81.66
TC 00001		84.65
TC 00002		72.96
TC 00010		51.87
BD 00000		86.11
BD 00001		92.36
BD 00002		87.07

Table 8. Experimental results for the MR8 filter bank.

Database	Method	Accuracy [%]
TC 00000	MR8 - Filtering	70.41
TC 00001		70.64
TC 00002		56.90
TC 00010		72.57
BD 00000		91.66
BD 00001		88.88
BD 00002		86.90

The results depicted in Tables 7 and 8 indicate that sampling the texture properties using a large bank of filters is unjustified and this observation is supported both by our experimental results and the findings reported in Varma and Zisserman (Varma and Zisserman, 2003). Our studies show that the texture orientation is the dominant textural property and this observation is supported by the fact that optimal classification results are obtained when the texture features are calculated using approaches such as standard LBP and Gabor filtering (when the frequency parameter of the Gabor filter is set to large values) that are specifically designed to record the image orientation for each pixel in the image. In our experiments (see Tables 7 and 8), the texture analysis approach based on filtering the image data using MR8 filters outperformed the LM filter banks when applied to Brodatz databases (due to their isotropic characteristics) and to Outex TC 00010 that is constructed using rotated textures.

4. Discussions on the Reported Results

The experimental results depicted in Section 3 were carried out in order to evaluate the performance of the LBP techniques when compared to the performance offered by texture analysis techniques based on filtering the image with a set of directional (Gabor), isotropic (S-Filters) filters and filter banks constructed using a large number of oriented and isotropic filters such as LM and MR8. Based on this analysis, we can conclude that the multi-channel S-Filtering technique is not suitable for the classification of oriented textures, but it offers reasonable discrimination when applied to the classification of isotropic textures. Thus, this technique can be successfully applied to extract omni-directional texture models that can be used in the development of applications including image retrieval (Schmid, 2001). Better results are obtained by the texture analysis techniques based on LM and MR8 filter banks, but their use for texture classification is not justified since their performance proved to be lower than that offered by the LBP and Gabor texture analysis techniques.

The most important finding resulting from this study is that although the LBP/C and the multi-channel Gabor filtering techniques approach texture analysis from a different perspective, they have some similar characteristics. For instance, by modelling the Gabor filter bank to favour the extraction of high frequencies from the input image we obtain a filter set that responds strongly to texture orientation, a property that is also shared by the standard LBP/C texture descriptor. Conversely, by modelling the Gabor filter set to favour the extraction of low frequencies, the filter set becomes omni-directional and this is similar to the uniformity concept that is enforced when the rotational invariant LBP texture descriptors are calculated. At this stage we can conclude that the classification accuracy offered by the LBP texture descriptors is marginally higher than the performance offered by the multi-channel Gabor texture analysis, but it is useful to note that in this study we have not optimized the spectral selectivity of the filter banks. Hence, we conclude that the performances in texture classification offered by the LBP/C and multi-channel Gabor filtering are comparable.

Arising from these results, it would be useful to examine whether the LBP/C texture descriptors and multi-channel Gabor filtering technique complement each other. To answer this question we need to evaluate the classification accuracy for each texture in the database and to analyse if one technique clearly

outperforms the other when classifying a particular texture. This analysis is illustrated in Table 9 where the distribution of the misclassified images for each class is depicted. From this table it can be observed that the classification errors for all investigated techniques are highest for texture classes 9, 15 and 17-21, a fact that further reinforces the main conclusion resulting from this study, namely the similarity between the texture analysis principles that are employed by the LBP and Gabor-based filtering methods in the process of sampling textural properties.

Table 9. Distribution of misclassified textures for LBP and Gabor techniques described in Section 2 (database TC00000)

Method	0	1	2	3	4	5	6	7	8	9	10	11	12	13	14	15	16	17	18	19	20	21	22	23
LBP/C Bins 4																								
LBP/C Bins 8																								
LBP/C Bins 16										2								3						
LBP^{ri}_{8}			1							1				1	3		1	2	1	4	1	1	2	
LBP^{ri}_{16}			1	1						2			1	1	3	3	1	2	5	2	4		3	
LBP^{ri}_{24}	1	1	2	1						5		1	2		3	3		2	1	2	3	1	3	2
GF1.0/2π 4 angles	1	1								4					4	3	1	6	1	2	5	4		2
GF1.5/2π 4 angles	1			1						3					2			2	1	2	1	5		1
GF2.0/2π 4 angles										2							1	2	2	2				
GF2.5/2π 4 angles										2								3	1					
GF1.0/2π 6 angles	1	1								4					4	3	1	6	2	3	3	4		1
GF1.5/2π 6 angles	1			1						2					2		1	2		2	2	3		1
GF2.0/2π 6 angles										1							1	2	2	1				
GF2.5/2π 6 angles										1								3						

5. Conclusions

The main goal of this investigation was to perform a comparative study where the performances in texture classification offered by the Local Binary Patterns (LBP) and multi-channel filtering techniques are analysed. In this study the effects of the variation in image size and texture rotation on the classification results have been evaluated. In this regard, we have conducted the experiments using four Outex databases defined by 24 texture classes and three Brodatz databases defined by 36 texture classes

and the classification results indicate that the performances of the LBP technique and multi-channel Gabor filtering are comparable. Our experimental results strengthen the conclusion that orientation is an important characteristic of the texture and best results are achieved when this texture property is accurately sampled by the texture descriptors (this conclusion is also confirmed by the results reported in our recent papers where the discriminative power of two texture analysis techniques based on the evaluation of the local image orientation at different observation scales (Ilea et al, 2008; Ghita et al, 2008) was quantitatively measured when the analysed techniques were applied for texture classification tasks). Another important finding resulting from this investigation is the fact that although the concepts behind the LBP and multi-channel filtering techniques are different, we have demonstrated that their behaviour in modelling oriented and isotropic textures shares many similarities. This is motivated in part by the fact that both approaches analyse the texture at a micro-level by either performing the calculation of the texture descriptor in a small neighbourhood or by performing pixel-wise filtering while the texture spectrum is defined at a macro-level by the distribution of the calculated texture units.

References

Balas, B. (2006), "Texture synthesis and perception: Using computational models to study texture representations in the human visual system", *Vision Research*, vol. 46, pp. 299-309.

Bergen, J. and Adelson, E. (1988), "Early vision and texture perception", *Nature*, vol. 333, pp. 363-364.

Bovik, A.C., Clark, M. and Geisler, W.S. (1990), "Multichannel texture analysis using localized spatial filters", *IEEE Transactions on Pattern Analysis and Machine Intelligence*, vol. 12, no. 1, pp. 55-73.

Brodatz, P. (1966), *Textures: A Photographic Album for Artists and Designers*, Dover Publications, New York.

Chang, C. and Lin, C.J. (2001), "LIBSVM: A library for support vector machines", http://www.csie.ntu.edu.tw/~cjlin/libsvm.

Chellappa, R., Kashyap, R.L. and Manjunath, B.S. (1998), "Model based texture segmentation and classification", in C.H. Chen, L.F. Pau and P.S.P Wang (Eds.), The Handbook of Pattern Recognition and Computer Vision, World Scientific Publishing.

Coggins, J.M. and Jain, A.K. (1985), "A spatial filtering approach to texture analysis", *Pattern Recognition Letters*, vol. 3, pp. 195-203.

Cula, O.G. and Dana, K.J. (2004), "3D texture recognition using bi-directional feature histograms", *International Journal of Computer Vision*, vol. 59, no. 1, pp. 33-60.

Daugman, J.G. (1988), "Complete discrete 2D Gabor transforms by neural networks for image analysis and compression", *IEEE Transactions on Acoustics, Speech and Signal Processing*, vol. 36, no. 7, pp. 1169-1179.

Dunn, D., Higgins, W. and Wakeley, J. (1994), "Texture segmentation using 2D Gabor elementary functions", *IEEE Transactions on Pattern Analysis and Machine Intelligence*, vol. 16, no. 2, pp. 130-149.

Dunn, D. and Higgins, W., "Optimal Gabor filters for texture segmentation", *IEEE Transactions on Image Processing*, vol. 4, no. 7, pp. 947-964, 1995.

Dyer, C.R., Hong, T. and Rosenfeld, A. (1980), "Texture classification using gray level co-occurrence based on edge maxima", *IEEE Transactions on Systems, Man, and Cybernetics*, vol. 10, pp. 158-163.

Ghita, O., Whelan, P.F., Carew, T., and Nammalwar, P. (2005), "Quality grading of painted slates using texture analysis", *Computers in Industry*, vol. 56, no. 8-9, pp. 802-815.

Ghita, O., Whelan, P.F. and Ilea, D.E. (2008), "Multi-resolution texture classification based on local image orientation", in *Proc of the 5th International Conference on Image Analysis and Recognition* (ICIAR 2008), *Lecture Notes in Computer Science*, vol. 5112, Springer, Heidelberg, pp. 688-696.

Haley, G.M. and Manjunath, B.S. (1999), "Rotation-invariant texture classification using a complete space–frequency model", *IEEE Transactions on Image Processing*, vol. 8, no. 2, pp. 255-269.

Haralick, R.M. (1979), "Statistical and structural approaches to texture", in *Proc of IEEE*, vol. 67, pp. 786-804.

Ilea, D.E. and Whelan, P.F. (2008), *"*CTex - An adaptive unsupervised segmentation algorithm based on color-texture coherence", *IEEE Transactions on Image Processing*, vol. 17, no. 10, pp. 1926-1939.

Ilea, D.E., Ghita, O. and Whelan, P.F. (2008), "Evaluation of local orientation for texture classification", in *Proc. of the 3rd International Conference on Computer Vision Theory and Applications*, VISAPP 2008, vol. 1, Funchal, Portugal, pp. 357-364.

Jain, A.K. and Farrokhnia, F. (1991), "Unsupervised texture segmentation using Gabor filtering", *Pattern Recognition*, vol. 33, no.12, pp. 1167-1186.

Julesz, B. (1981), "Textons, the elements of texture perception, and their interactions", *Nature*, vol. 290, pp. 91-97.

Kachouie, N. and Alirazae, J. (2005), "Optimised multichannel filter bank with flat frequency response for texture segmentation", *EURASIP Journal on Applied Signal Processing*, vol. 12, no. 1, pp. 1834-1844.

Kamarainen, J.K., Kyrki, V. and Kalviainen, H. (2006), "Invariance properties of Gabor filter-based features-overview and applications", *IEEE Transactions on Image Processing*, vol. 15, no. 5, pp. 1088-1099.

Kovalev, V.A., Kruggel, F., Gertz, H.J. and von Cramon, D.Y. (2001), "Three-dimensional texture analysis of MRI brain datasets", *IEEE Transactions on Medical Imaging*, vol. 20, no. 5, pp. 424-433.

Lahajnar, F. and Kovacic, S. (2003), "Rotation-invariant texture classification", *Pattern Recognition Letters*, vol. 24, no. 9-10, pp. 1141-1161.

Leung, T. and Malik, J. (2001), "Representing and recognizing the visual appearance of materials using three-dimensional textons", *International Journal of Computer Vision*, vol. 43, no. 1, pp. 29-44.

Liu, X. and Wang, D. (2003), "Texture classification using spectral histograms", *IEEE Transactions on Image Processing*, vol. 12, no. 6, pp. 661-670.

Mäenpää, T., Viertola, J. and Pietikäinen, M. (2003), "Optimising colour and texture features for real-time visual inspection", *Pattern Analysis and Applications*, vol. 6, no. 3, pp. 169-175.

Mallat, S.G. (1989), "A theory for multiresolution signal decomposition: The wavelet representation", *IEEE Transactions on Pattern Analysis and Machine Intelligence*, vol. 11, no. 7, pp. 674-693.

Manjunath, B.S. and Ma, W.Y. (1996), "Texture features for browsing and retrieval of image data", *IEEE Transactions on Pattern Analysis and Machine Intelligence*, vol. 18, no. 8, pp. 837- 842.

Materka, A. and Strzelecki, M (1998), "Texture analysis methods – A review", *Technical Report*, University of Lodz, Cost B11 Report.

Nammalwar, P., Ghita, O. and Whelan, P.F. (2003), "Experimentation on the use of chromaticity features, Local Binary Pattern and Discrete Cosine Transform in colour texture analysis", in *Proc. of the Scandinavian Conference on Image Analysis* (SCIA 2003), Goteborg, Sweden, pp. 186-192.

Nammalwar, P., Ghita, O. and Whelan, P.F. (2010), "A generic framework for colour texture segmentation", *Sensor Review*, vol. 30, no. 1, pp. 69-79.

Ojala, T., Pietikäinen, M. and Harwood, D. (1994), "Performance evaluation of texture measures with classification based on Kullback discrimination of distributions", in *Proc. of the International Conference on Pattern Recognition* (ICPR), Jerusalem, Israel, pp. 582-585.

Ojala, T., Valkealahti, K. and Pietikäinen, M. (2001), "Texture discrimination with multidimensional distributions of signed gray-level differences", *Pattern Recognition*, vol. 34, no. 3, pp. 727-739.

Ojala, T., Pietikainen, M. and Maenpaa, T. (2002a), "Multiresolution gray-scale and rotation invariant texture classification with Local Binary Patterns", *IEEE Transactions on Pattern Analysis and Machine Intelligence*, vol. 24, no. 7, pp. 971-987.

Ojala, T., Mäenpää, T., Pietikäinen, M., Viertola, J., Kyllonen, J. and Huovinen S. (2002b), "Outex – a new framework for empirical evaluation of texture analysis algorithms", in *Proc. of the 16th International Conference on Pattern Recognition* (ICPR 2002), vol. 1, Quebec, Canada, pp. 701–706.

Petrou, M. and Sevilla, P.G. (2006), *Image Processing: Dealing with Texture*, John Wiley & Sons.

Porter, R. and Canagarajah, N. (1997), "Robust rotation-invariant texture classification: Wavelet, Gabor filter and GMRF based schemes", *IEE Proceedings - Vision, Image, and Signal Processing*, vol. 144, no. 3, pp. 180-188.

Randen, T. and Husoy, J.H. (1999a), "Texture segmentation using filters with optimized energy separation", *IEEE Transactions on Image Processing*, vol. 8, no. 4, pp. 571-582.

Randen, T. and Husoy, J.H. (1999b), "Filtering for texture classification: A comparative study", *IEEE Transactions on Pattern Analysis and Machine Intelligence*, vol. 21, no. 4, pp. 291-310.

Rodriguez, Y. and Marcel, S. (2006), "Face authentication using adapted Local Binary Pattern histograms", in *Proc. of the 9th European Conference on Computer Vision* (ECCV 2006), Graz, Austria, vol. 4, pp. 321-332.

Schmid, C. (2001), "Constructing models for content-based image retrieval", in *Proc. of the IEEE Conference on Computer Vision and Pattern Recognition* (CVPR 2001), vol. 2, pp. 39-45.

Tsatsanis, M.K. and Giannakis, G.B. (1992), "Object and texture classification using higher order statistics", *IEEE Transactions on Pattern Analysis and Machine Intelligence*, vol. 14, no. 7, pp. 733-750.

Tosun, A.B. and Gunduz-Demir, C. (2011), "Graph run-length matrices for histopathological image segmentation", *IEEE Transactions on Medical Imaging*, vol. 30, no. 3, pp. 721-732.

Tuceryan, M. and Jain, A.K. (1998), "Texture analysis", in C.H. Chen, L.F. Pau and P.S.P. Wang (Eds.), The Handbook of Pattern Recognition and Computer Vision, World Scientific Publishing.

Valkealahti, K. and Oja, E. (1998), "Reduced multidimensional co-occurrence histograms in texture classification", *IEEE Transactions on Pattern Analysis and Machine Intelligence*, vol. 20, no. 1, pp. 90-94.

Varma, M. and Zisserman, A. (2002), "Classifying images of materials: Achieving viewpoint and illumination independence", in *Proc. of the 7th European Conference on Computer Vision* (ECCV 2002), Copenhagen, Denmark, 2002.

Varma, M. and Zisserman, A. (2003), "Texture classification: Are filter banks necessary?", in *Proc. of the IEEE Conference on Computer Vision and Pattern Recognition* (CVPR 2003), vol. 2, pp. 691-698.

Varma, M. and Zisserman, A (2004), "Unifying statistical texture classification frameworks", *Image and Vision Computing*, vol. 22, no. 14, pp. 1175-1183.

Weber, D.M. and Casasent, D.P. (2001), Quadratic Gabor filters for object detection", *IEEE Transactions on Image Processing*, vol. 10, no. 2, pp. 218-230.

Weszka, J.S., Dyer, C.R. and Rosenfeld, A. (1976), "A comparative study of texture measures for terrain classification", *IEEE Transactions on Systems, Man and Cybernetics*, vol. 6, pp. 269-285.

Xie, X. and Mirmehdi, M. (2007), “TEXEMS: Texture exemplars for defect detection on random textured surfaces”, *IEEE Transactions on Pattern Analysis and Machine Intelligence*, vol. 29, no. 8, pp. 1454-1464.

Zhang, J., and Tan, T. (2002), “Brief review of invariant texture analysis methods”, *Pattern Recognition*, vol. 35, no. 3, pp. 735-747.